A NEW METRIC FOR ROUTING IN MULTI-HOP WIRELESS SENSOR NETWORKS FOR DETECTION OF CORRELATED RANDOM FIELDS

Youngchul Sung and Lang Tong[†]

Electrical and Computer Engineering
Cornell University
Ithaca, NY 14850
Email:{ys87,ltong}@ece.cornell.edu

Anthony Ephremides

Dept. of Electrical Engineering
University of Maryland
College Park, MD 20742
Email:tony@eng.umd.edu

ABSTRACT

The problem of combining task performance and routing for the detection of correlated random fields using multi-hop wireless sensor networks is considered. Under the assumption of Gauss-Markov structure along a given route, a link metric that captures the detection performance associated with a route is derived. Under Bayesian formulation Chernoff information is used as a performance criterion. It is shown that at high SNR Chernoff information is approximately given by a sum of the logarithm of the innovation variance at each link, which thus provides a link metric to determine the optimal route for the detection application. The value of the proposed metric is equivalent to the mutual information for Gaussian channel with signal power defined as the variance of signal innovation. The properties of the proposed metric are also investigated. It is shown that for SNR > 1, as a function of link length, the metric is 1) strictly increasing, 2) strictly concave, 3) bounded from above and the maximum information that a link can provide is $\frac{1}{2}\log(1+\text{SNR})$ achieved by independent and identically distributed samples. It is also shown that the proposed link metric is well approximated by a function of the length of the corresponding link only.

1. INTRODUCTION

Many criteria have been proposed to select the optimal route in multi-hop wireless networks. Typical link metric includes the hop count, minimum delay, traffic amount, etc. For energy-limited wireless networks different metric such as the battery power of nodes, necessary transmission power between neighboring nodes, has also been considered to maximize the network lifetime by distributing routes evenly over the network [1, 2, 3, 4]. However, the main purpose of sensor networks lies in specific applications such as detection, monitoring, estimation, etc., using collaborative processing between sensor nodes, whereas conventional wireless *ad hoc* networks focus on the communication between nodes. Hence, it is desirable to incorporate the application performance into routing in sensor networks. Examples of such cross-layer approach are found in [5, 6, 7, 8, 9].

In this paper, we consider a cross-layer approach to combine the detection performance with routing to a gateway node in large sensor networks. We consider a specific application, that is, detection of spatially correlated random fields using networked sensors deployed over a geographical region, where each sensor on a route to the gateway node receives the data from a neighboring sensor and also makes its own measurement of a phenomenon at its location. The assumption of spatial correlation is proper for large sensor networks, especially for densely deployed networks. While the geometry of a route to the gateway node is irrelevant for commonly assumed independent and identically distributed (i.i.d.) signal fields, the spatial correlation affects the performance of detection based on different routes even if the number of sensors on routes are the same. In [10], we have proposed a new link metric that captures the detection performance along a fusion route based on the innovations approach [11] to calculation of Chernoff information associated with a fusion route under state-space signal and observation model. Here, we further investigate the properties of the proposed link metric and provide some simulation results.

First, we show that the new link metric, logarithm of the variance of innovation of observation sequence, is equivalent to the capacity for Gaussian channel with signal power defined as the variance of signal innovation. Second, we show that for SNR $>$ 1, as a function of link length, the metric is 1) strictly increasing, 2) strictly concave, 3) bounded from above and converging to $\frac{1}{2}\log(1+\text{SNR})$ as the link length increases unboundedly. Thus, the maximum performance gain per link is achieved by i.i.d. observations for SNR > 1. Third, we also show that the performance difference by route geometry is not significant when SNR is very low.

The remainder of the paper is organized as follows. In Section 2 we describe the data model. In Section 3 we investigate the properties of the proposed metric for the detection performance. Simulation results are given in Section 4, followed by conclusion in Section 5.

2. SYSTEM MODEL

We consider the detection of a correlated random field $\mathcal{S}$ over a two-dimensional space $\mathcal{X}$ using wireless networked sensors deployed over the space under the Bayesian formulation, where the hypotheses H_1 and H_0 represent the presence of signal $\mathcal{S}$ and the event of no signal over $\mathcal{X}$, respectively. We assume that the signal field is static during the period of observation and processing. We also assume that each sensor knows its own location and sensor observations are delivered via multi-hop routes to a gateway node

[†]This work was supported in part by the Multidisciplinary University Research Initiative (MURI) under the Office of Naval Research Contract N00014-00-1-0564. Prepared through collaborative participation in the Communications and Networks Consortium sponsored by the U. S. Army Research Laboratory under the Collaborative Technology Alliance Program, Cooperative Agreement DAAD19-01-2-0011. The U.S. Government is authorized to reproduce and distribute reprints for Government purposes notwithstanding any copyright notation thereon.

where the final decision is made. Since sensors are located within the signal field (if H_1 would occur), each sensor on a route to the gateway node not only transfers data from the previous sensor but also makes its own observation (corrupted by measurement noise) and delivers the aggregated data to the next sensor on the route. Thus, data fusion occurs along the route to the gateway node.

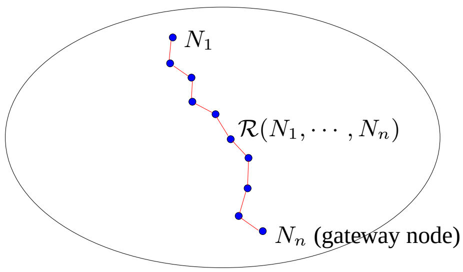

Fig. 1. Detection along a fusion route.

Consider a fusion route traversing sensor nodes $N_1, N_2, \cdots, N_n$, as shown in Fig. 1, where N_n is the gateway node and N_1 is the node starting the fusion process. Let $\mathcal{R}(N_1, \cdots, N_n)$ denote this fusion route. We make the following assumption on the correlation structure of the random field $\mathcal{S}$.

A 1 *For any open simple route $\mathcal{R}$ traversing an arbitrary set of nodes contained in $\mathcal{X}$, the signal along the route forms an one-dimensional stationary Gauss-Markov process and the signal model is given by*

$$\frac{ds(l)}{dl} = -As(l) + Bu(l), \quad 0 \le l \le |\mathcal{R}|, \tag{1}$$

where $|\mathcal{R}|$ denotes the length of the route $\mathcal{R}$, $A \ge 0$ and B are known, and the initial condition is given by $s(0)$ which has Gaussian distribution $\mathcal{N}(0, \Pi_0)$ with $\Pi_0 = \frac{B^2}{2A}$. The process noise $u(l)$ is zero-mean white Gaussian with unit variance, independent of both $s(0)$ and the measurement noise of sensor.

Here, A represents the diffusion rate of the signal field with respect to distance. Assumption 1 may be an oversimplification for general correlation and curve shapes. However, it makes analytic development tractable, and is reasonable for a class of curves that are almost straight contained in a homogeneous Gauss-Markov random field.

Since each sensor makes an observation of the signal process at its location, the observation along $\mathcal{R}(N_1, \cdots, N_n)$ is given by

$$\begin{array}{lll} H_0 & : & y_i = w_i, \\ H_1 & : & y_i = s_i + w_i, \quad i = 1, 2, \cdots, n, \end{array} \tag{2}$$

where y_i is the observation at node N_i located at $\mathbf{x}_i$, $s_i \triangleq s(\mathbf{x}_i)$, and w_i are i.i.d. sensor measurement noises from $\mathcal{N}(0, \sigma^2)$ with a known variance σ^2. The prior probabilities of H_0 and H_1 are given by π_0 and π_1, respectively. Under Assumption 1 the dynamics of signal sample s_i at node N_i is described by the following state-space model:

$$\begin{aligned} s_{i+1} &= a_i s_i + u_i, \\ a_i &= e^{-A\Delta_i}, \\ u_i &\sim \mathcal{N}(0, \Pi_0(1 - a_i^2)), \end{aligned} \tag{3}$$

where the distance between two neighboring sensors on the route $\Delta_i = ||\mathbf{x}_{i+1} - \mathbf{x}_i||$.

3. PERFORMANCE METRIC AND PROPERTIES

Since we are interested in the detection performance, we consider as a figure of merit the average error probability of optimal detection based on a fusion route. However, the exact calculation of error probability is not available for general Gauss-Markov signals [12]. Thus, a link metric has been derived based on Chernoff bound [13] on the error probability based on the model (2, 3) in [10]. The derived performance metric is designed to minimize the Chernoff (upper) bound on the average error probability satisfying additivity condition[1] using the innovations approach [11] to log-likelihood calculation.

3.1. Background

Here, we summarize the results in [10]. (For detailed derivation, see the reference.) Consider a fusion route $\mathcal{R}(N_1, \cdots, N_n)$. The Chernoff bound on the average error probability of the MAP detector is given by [12]

$$P_e = \pi_0 P(\mathcal{E}|H_0) + \pi_1 P(\mathcal{E}|H_1) \le \pi_0^{1-s} \pi_1^s e^{\mu_{T,0}(s)}, \tag{4}$$

where $0 \le s \le 1$ and $\mu_{T,0}$ is the cumulant generating function of the log-likelihood ratio $T \triangleq \log \frac{p_1(y_1^n)}{p_0(y_1^n)}$ under H_0, i.e.,

$$\mu_{T,0}(s) = \log \mathbb{E}_0 \left\{ e^{s \log \frac{p_1(y_1^n)}{p_0(y_1^n)}} \right\}, \quad y_1^n \triangleq \{y_1, \cdots, y_n\}. \tag{5}$$

Chernoff information between $p_0(y_1^n)$ and $p_1(y_1^n)$ is defined as the exponent in (4) yielding the tightest bound, i.e.,

$$C\left(p_0(y_1^n), p_1(y_1^n)\right) \triangleq \sup_{0 \le s \le 1} \{-\mu_{T,0}(s)\} \tag{6}$$

Using the innovations representation for $\log p_1(y_1^n)$ and $\log p_0(y_1^n)$ [10, 11], we have

$$\begin{aligned} \mu_{T,0}(s) \;=\; & \log \mathbb{E}_0 \Bigg\{ \exp \Bigg[s \Bigg(-\frac{1}{2} \sum_{i=1}^n \log R_{e,i} - \frac{1}{2} \sum_{i=1}^n \frac{e_i^2}{R_{e,i}} \\ & + \frac{n}{2} \log \sigma^2 + \frac{1}{2\sigma^2} \sum_{i=1}^n y_i^2 \Bigg) \Bigg] \Bigg\}. \end{aligned} \tag{7}$$

Since the variance $R_{e,i}$ of innovation of observation is deterministic, $\frac{1}{n} \sum_{i=1}^n y_i^2$ converges almost surely to its mean $\sigma^2 (= \mathbb{E}_0\{y_i^2\})$ under H_0 by the strong law of large numbers (SLLN) as n increases, and $\frac{e_i^2}{R_{e,i}}$ converges to zero in mean square sense as SNR increases, the Chernoff information at high SNR is attained at $s^* \approx 1$ and is given by

$$\begin{aligned} C\left(p_0(y_1^n), p_1(y_1^n)\right) &\approx \frac{1}{2} \left\{ \sum_{i=0}^{n-1} \log R_{e,i} - n(\log \sigma^2 + 1) \right\} \\ &= \frac{1}{2} \left\{ \sum_{i=0}^{n-1} \left(\log \frac{R_{e,i}}{\sigma^2} - 1 \right) \right\}, \end{aligned} \tag{8}$$

for sufficiently large n. Since the constant term does not depend on link length, at high SNR a link metric that captures Chernoff information at link i is given by

$$C_i \triangleq \frac{1}{2} \log \frac{R_{e,i}}{\sigma^2}. \tag{9}$$

[1] The overall metric is decomposed as a sum of contribution of each link to the performance.

Thus, Chernoff information provided by a fusion route is approximated by the sum of the logarithm of the innovation variance at each link, and the logarithm of the variance of normalized innovation (of observation) can be used as a link metric. Since e_i has Gaussian distribution $\mathcal{N}(0, R_{e,i})$, the entropy of the innovation e_i at link i is given by $\frac{1}{2}\log(2\pi e R_{e,i})$. Hence, the optimal route in our metric maximizes the accumulated entropy of the innovation process along the route.

3.2. Properties of the link metric

First, it is straightforward to see that the link metric C_i is equivalent to the channel capacity of Gaussian channel with modified signal power, i.e.,

$$C_i = \frac{1}{2}\log\frac{R_{e,i}}{\sigma^2} = \frac{1}{2}\log\left(1+\frac{P_{i|i-1}}{\sigma^2}\right), \tag{10}$$

since $R_{e,i} = \sigma^2 + P_{i|i-1}$ [14], where the variance of signal innovation $P_{i|i-1} \triangleq \mathbb{E}(s_i - \hat{s}_{i|i-1})^2$ and $\hat{s}_{i|i-1}$ is the minimum mean square estimate of s_i given $\{y_1, \cdots, y_{i-1}\}$. The relationship between Chernoff information per link and Gaussian channel capacity is clear; at high SNR Chernoff information per link is equivalent to the Gaussian channel capacity with signal power defined by the variance $P_{i|i-1}$ of signal innovation. Since $0 \le P_{i|i-1} \le \Pi_0$ and the maximum $\Pi_0(= \mathbb{E}\{s_i^2\})$ is attained by independent signal samples, we can see that the correlation always reduces Chernoff information at high SNR.

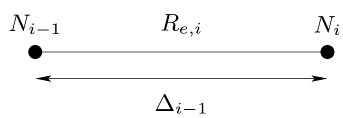

Fig. 2. Link i.

Now, we investigate the properties of the proposed metric as a function of link length. An explicit formula for the link metric C_i as function of link length Δ_{i-1} is obtained using Kalman recursion.

Proposition 1 *The link metric C_i as a function of link length Δ_{i-1} is given by*

$$C_i(\Delta_{i-1}) = \frac{1}{2}\log\left\{1+SNR-(SNR-K_{i-1})e^{-2A\Delta_{i-1}}\right\}, \tag{11}$$

where $K_{i-1} \triangleq \frac{P_{i-1|i-2}}{P_{i-1|i-2}+\sigma^2}$ $(0 \le K_{i-1} \le 1)$ is a constant with respect to the current link length Δ_{i-1}.

Proof: A recursion for the signal innovation variance (MMSE prediction error) is given by

$$P_{i|i-1} = \frac{\sigma^2 a_{i-1}^2 P_{i-1|i-2}}{P_{i-1|i-2}+\sigma^2} + Q_{i-1}, \tag{12}$$

where $Q_{i-1} = \Pi_0(1-a_{i-1}^2)$ and $P_{i-1|i-2}$ depends only on the previous links $\{\Delta_1, \cdots, \Delta_{i-2}\}$. Thus, we have

$$\begin{aligned} R_{e,i} &= \sigma^2 + P_{i|i-1} = \sigma^2 + \sigma^2 a_{i-1}^2 \frac{P_{i-1|i-2}}{P_{i-1|i-2}+\sigma^2} + Q_{i-1}, \\ &= \sigma^2 + \Pi_0 - (\Pi_0 - \sigma^2 K_{i-1})e^{-2A\Delta_{i-1}}, \end{aligned} \tag{13}$$

where (13) is obtained by substituting $a_{i-1} = e^{-A\Delta_{i-1}}$. Hence, from (10) the metric for link i is given by (11). ■

Furthermore, at high SNR we have $K_{i-1} \approx 1$, and the proposed metric is approximated by

$$C_i \approx \hat{C}_i \triangleq \frac{1}{2}\log\left\{1+\text{SNR}-(\text{SNR}-1)e^{-2A\Delta_{i-1}}\right\}. \tag{14}$$

Notice that $\hat{C}_i$ depends only on the current link length Δ_{i-1}, which makes the calculation of accumulated metric simple. Numerical results show that the exact metric is well approximated by $\hat{C}_i$ at reasonably high SNR. Figure 3 shows the value of C_i as a function of link length. It is seen that C_i increases monotonically as Δ_{i-1} increases and converges eventually. The properties of C_i as a function of link length is summarized in the following theorem.

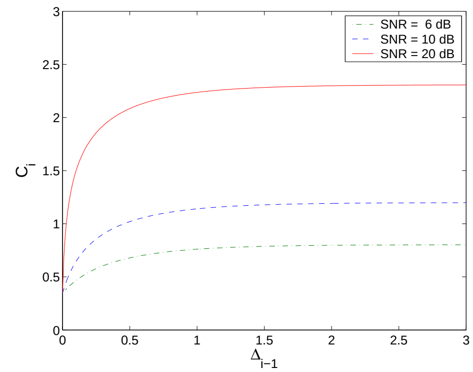

Fig. 3. C_i versus Δ_{i-1} $(A = 1, K_{i-1} = 1)$.

Theorem 1 *For a given set $\{\Delta_1, \cdots, \Delta_{i-2}\}$ of previous link lengths and SNR > 1, the link metric C_i has the following properties:*

- *(i) It is nonnegative and a strictly increasing function of Δ_{i-1},*
- *(ii) converges to $\frac{1}{2}\log(1+SNR)$ exponentially as Δ_{i-1} increases,*
- *(iii) and the function is strictly concave.*

The approximated metric $\hat{C}_i$ has the same properties.

Proof: From (11) the convergence to $\frac{1}{2}\log(1+\text{SNR})$ regardless of the value of K_{i-1} and its rate are straightforward since $\lim_{x\to\infty}\frac{\log c_1 - \log(c_1 - c_2 e^{-x})}{e^{-x}} = c_2/c_1$ for $c_1 > c_2 > 0$. The partial derivative of C_i with respect to Δ_{i-1} is given by

$$\frac{\partial C_i}{\partial \Delta_{i-1}} = \frac{A(\text{SNR}-K_{i-1})e^{-2A\Delta_{i-1}}}{\text{SNR}+1-(\text{SNR}-K_{i-1})e^{-2A\Delta_{i-1}}}. \tag{15}$$

Since $0 \le K_{i-1} \le 1$, SNR > 1 implies $\frac{\partial C_i}{\partial \Delta_{i-1}} > 0$ and the link metric is a strict increasing function of Δ_{i-1}. The second partial derivative is given by

$$\frac{\partial^2 C_i}{\partial \Delta_{i-1}^2} = \frac{-2A^2(\text{SNR}+1)(\text{SNR}-K_{i-1})e^{-2A\Delta_{i-1}}}{(\text{SNR}+1-(\text{SNR}-K_{i-1})e^{-2A\Delta_{i-1}})^2}. \tag{16}$$

Therefore, for SNR > 1, $\frac{\partial^2 C_i}{\partial \Delta_{i-1}^2} < 0$ and the metric is a strictly concave function of Δ_{i-1}. For $\hat{C}_i$, $K_{i-1} \equiv 1$, and the claim follows. ■

The strict concavity of the metric C_i and $\hat{C}_i$ as a function of link length is important, and makes the optimization problem simple. For example, consider sensor placement problem where we want to optimize sensor spacing to maximize the detection performance over some feasible set $\{(\Delta_1, \cdots, \Delta_{n-1}) : f(\Delta_1, \cdots, \Delta_{n-1}) \le c\}$. (For example, total transmission energy constraint is represented by $f(\Delta_1, \cdots, \Delta_{n-1}) = \sum_{i=1}^{n-1} \Delta_i^2$.) In particular, if we use $\hat{C}_i$, this problem reduces to a separable convex optimization problem due to the concavity of $\hat{C}_i$ from Theorem 1 and convexity of the feasible set satisfying total energy or length constraint. It is easy to show that uniform spacing results in maximal total Chernoff information. One can argue that uniform placement is also optimal using the exact metric C_i at high SNR since C_i converges to $\hat{C}_i$ as SNR increases. (However, uniform placement is not optimal when SNR is very low or the field correlation is very strong.)

The maximal information that a link can provide is given by

$$C_{max} = \frac{1}{2}\log(1 + \text{SNR}), \tag{17}$$

achieved at $\Delta_{i-1} = \infty$ (i.e., the next sample is independent of all the previous samples) regardless of the value of K_{i-1}. For a finite Δ_{i-1} with SNR > 1 the information is reduced from C_{max} due to the correlation between two samples at neighboring sensors. However, with a finite Δ_{i-1} we can achieve most of C_{max} due to the exponential convergence. It is worth noting that the maximal information that a link can provide is the same as the capacity of the Gaussian channel with i.i.d. channel uses at high SNR, which is dealt with in more detail in Section 3.3.

When the link length Δ_{i-1} approaches zero, on the other hand, the information for the link converges to $\frac{1}{2}\log(1 + K_{i-1})$. Note that $K_{i-1} > 0$ if $P_{i-1|i-2} > 0$, i.e., the estimation for s_{i-1} given $\{y_1, \cdots, y_{i-2}\}$ is not perfect. However, the accumulated information does not increases linearly with n.

Theorem 2 *If $\Delta_{i-1} = 0$ for all i, the total information increases at the rate of $\log\sqrt{n}$ as n increases and the average information per observation converges to zero.*

Proof: See [15] ∎

Now we define the detection efficiency η of a link as the information per unit energy, i.e.,

$$\eta \triangleq \frac{C_i}{E_i}, \tag{18}$$

where E_i is the required energy per link consisting of processing and transmission energy. Figure 4 shows the detection efficiency as a function of the link length Δ_{i-1} for $K_{i-1} = 1$ and several values of the processing energy E_p. Here, the inverse square law is used for wireless propagation, i.e., $E_i = E_p + \Delta_{i-1}^2$. It is seen that the information per unit energy initially increases as the link length increases, reaches a maximum, and then decreases to zero as the link length further increases. It is also seen that the most energy-efficient spacing Δ_{i-1}^* in terms of the detection performance is dependent on E_p, and is given by solving

$$\frac{\partial}{\partial \Delta_{i-1}} \left(\frac{\log\left\{1 + \text{SNR} - (\text{SNR} - K_{i-1})e^{-2A\Delta_{i-1}}\right\}}{E_p + \Delta_{i-1}^{\nu}} \right) = 0, \tag{19}$$

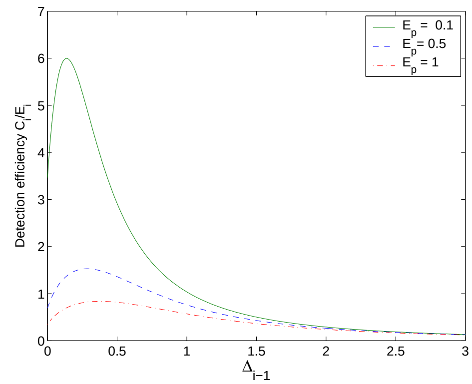

Fig. 4. Information per unit energy, $\frac{C_i}{E_i}$, versus Δ_{i-1} ($A = 1, K_{i-1} = 1$).

where ν is the attenuation coefficient for wireless propagation. Note that Δ_{i-1}^* can be used to determine the sensor density over space at the initial deployment phase to provide the sensor spacing that is most efficient in per-link detection performance in terms of energy consumption.

3.3. I.i.d. case

Now we consider the i.i.d. case to make a connection to the approximation at high SNR in the previous section. In the i.i.d. case ($a_i = 0, \ \forall\, i$), the exact computation of the Chernoff information is available. The Chernoff information between two joint distributions is given by

$$C(p_0(y_1, \cdots, y_n), p_1(y_1, \cdots, y_n)) = nC(p_0, p_1), \tag{20}$$

where

$$p_0 = \mathcal{N}(0, \sigma^2) \text{ and } p_1 = \mathcal{N}(0, \Pi_0 + \sigma^2), \tag{21}$$

$$C(p_0, p_1) = -\frac{1}{2}\log\left[\frac{1 + \text{SNR}}{\text{SNR}}\log(1 + \text{SNR})\right] + \frac{1 + \text{SNR}}{2\text{SNR}}\log(1 + \text{SNR}) - \frac{1}{2}, \tag{22}$$

and the optimal s^* for the tightest bound is given by

$$s^* = 1 + \frac{1}{\text{SNR}} - \frac{1}{\log(1 + \text{SNR})}. \tag{23}$$

Fig. 5 shows s^* as a function of SNR. As expected, it is seen from (23) that the optimal s^* converges to one as SNR increases. On the other hand, s^* converges to $\frac{1}{2}$ as the SNR decreases to zero. Thus, Bhattacharyya bound gives a tight upper bound at low SNR regime. The asymptotic (in SNR) behavior of Chernoff information is given by the following theorem.

Theorem 3 *The Chernoff information for the binary MAP detection for the null and alternative distributions (21) is equivalent to the Gaussian channel capacity $\frac{1}{2}\log(1 + SNR)$ asymptotically (in SNR), i.e.,*

$$\lim_{SNR \to \infty} \frac{C(p_0, p_1)}{\frac{1}{2}\log(1 + SNR)} = 1. \tag{24}$$

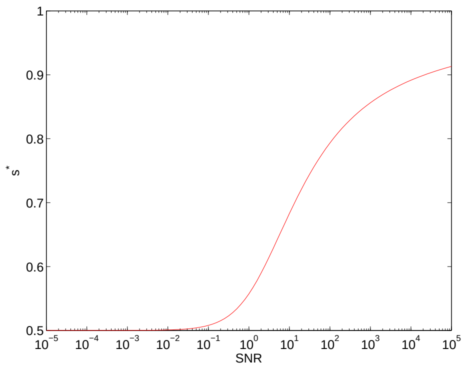

Fig. 5. Optimal parameter s^* minimizing Chernoff bound.

First, Theorem 3 establishes a relationship between the Chernoff information for the binary MAP detection of i.i.d. Gaussian signals in Gaussian noise and the Gaussian channel capacity. These two information measures are equivalent at high SNR. Second, comparing (8,10) and (22), we recognize what is involved in the approximation in the previous section. From the high SNR assumption, we have approximated $s^* \approx 1$ and neglected the term that increases with order of $-\frac{1}{2}\log[\log(1+\text{SNR})]$, which increases with slower rate than the dominant term $\frac{1}{2}\log(1+\text{SNR})$. Surprisingly, this approximation well predicts the relative detection performance based on different routes even when the SNR is not so high, as seen in Section 4. Theorem 3 provides a rationale for using (10) as a link metric at high SNR. The difference is that in the correlated case the signal power is defined by the variance of the *signal innovation* not by the variance of the signal itself. The information per link reduces to $\frac{1}{2}\log(1+\text{SNR})$ in the i.i.d. case since we have $\hat{s}_{i|i-1}=0$ and

$$\mathbb{E}\{s_i^2\} = \Pi_0 = P_{i|i-1} \triangleq \mathbb{E}\{(s_i - \hat{s}_{i|i-1})^2\}, \quad (25)$$

in this case.

3.4. Low SNR case

Up to now, we have shown that the logarithm of innovation variance $R_{e,i}$ at link i or equivalently $\frac{1}{2}\log\left(1+\frac{P_{i|i-1}}{\sigma^2}\right)$ can be used as a link metric that captures detection performance at high SNR and investigated its properties. The optimal selection of a route based on the proposed metric can significantly improve detection performance at high SNR, as shown in Section 4. However, at low SNR the performance difference among different routes with the same number of nodes is not as significant as in high SNR since the noise factor is dominant in the low SNR regime. We can see this easily by the Kalman recursion (26-29) for the innovation variance $R_{e,i}$. In the exponent of the cumulant generating function (7) we see that there are two terms depending on the route geometry: $\log R_{e,i}$ and $\frac{e_i^2}{R_{e,i}}$.

$$P_{1|0} = \Pi_0, \quad (26)$$

$$R_{e,i} = \sigma^2 + P_{i|i-1}, \quad (27)$$

$$K_{p,i} = a_i P_{i|i-1} R_{e,i}^{-1}, \;\; a_i = e^{-A\Delta_i}, \quad (28)$$

$$P_{i+1|i} = a_i^2 P_{i|i-1} + \Pi_0^2(1-a_i^2) - a_i^2 P_{i|i-1}^2 R_{e,i}^{-1}. \quad (29)$$

Consider the asymptotic case that SNR ($=\frac{\Pi_0}{\sigma^2}$) decreases to zero for a fixed large n. Here, we fix $\sigma^2 > 0$ and decrease the signal process variance Π_0 to zero. It is seen from (26-29) that $P_{i|i-1} \to 0$ for all $i = 1, \cdots, n$, as $\Pi_0 \to 0$. When $P_{i|i-1}$ becomes so small that the noise variance σ^2 in (27) is dominant, the change of $P_{i|i-1}$ due to the variation of link length is insignificant compared with σ^2 and consequently the change in $\log R_{e,i}$ is not as significant as in high SNR case. For the other term $\frac{e_i^2}{R_{e,i}}$, consider the following recursive filtering for e_i:

$$e_i = y_i - K_{p,i-1}y_{i-1} - (a_{i-1}-K_{p,i-1})K_{p,i-2}y_{i-2} - \cdots - (a_{i-1}-K_{p,i-1})\cdots(a_2-K_{p,2})K_{p,1}y_1. \quad (30)$$

From (26-29) we have that $K_{p,i} \to 0$ as $\Pi_0 \to 0$. Thus, at low SNR y_i is the dominant factor in the right-hand side of (30). Since the cumulant generating function (7) is calculated under the null hypothesis H_0, y_i is given by measurement noise w_i which is assumed to be i.i.d. over samples. Thus, at low SNR the distribution e_i under H_0 is determined by that of y_i and does not depend on the route geometry significantly.

4. NUMERICAL RESULT

In this section, we present some numerical results to validate our performance metric. We considered Bayesian detection of a random field satisfying Assumption 1. We used equal prior probabilities for H_0 and H_1, and set the diffusion rate A of the field to be one. Due to Assumption 1 we considered the relative distance between nodes along routes for the route geometry. We considered the on-demand detection initiated by the gateway node described described in [10]. We considered 50 possible routes all with 20 sensor nodes (19 hops). Assuming spatial Poisson sensor locations, we generated link lengths using the exponential distribution with unit mean independently over hops and different routes. From these 50 route realizations we selected three routes: the shortest path requiring minimum energy, the longest path consuming maximum energy, and the optimal path that maximized our performance metric.

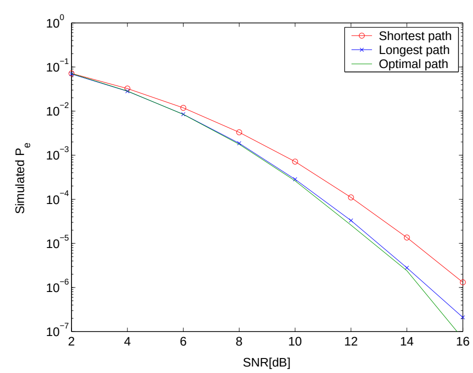

Fig. 6. Simulated average error probability P_e of three different routes

Figure 6 shows the simulated error probability of the MAP detector based on the three different routes with respect to SNR. It is seen that at low SNR the difference among three routes is not significant as expected. Nevertheless, the relative performance among the three routes is well preserved at low SNR according to the order predicted by our analysis based on high SNR. At high SNR, on the other hand, the performance difference is large. Note that the performance gain by the optimal metric is approximately 2 dB over the shortest route detection at high SNR, and this gain increases when the number of hops increases further. As expected, the performance of the optimal route in our metric provides the best performance. The longest route provided a better performance than the shortest since the expected innovation is large at links. However, the longest route does not necessarily provide the best performance since the performance also depends on the relative length among hops. Notice that our analysis based on large samples is valid only with 20 samples in this case.

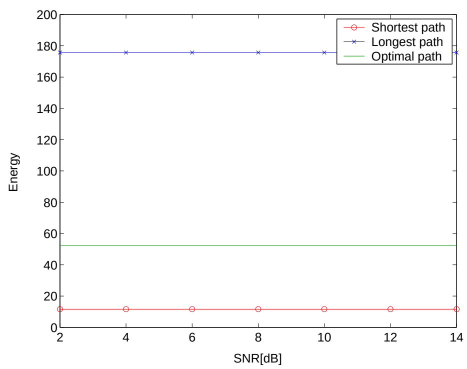

Fig. 7. Simulated average error probability P_e of three different routes

Figure 7 shows the total transmission energy required for the three routes without taking the processing energy into account. Assuming the inverse square law, we used Δ_i^2 as transmission energy. In the realization of 50 routes, we observed that one specific route remains as the optimal route for all the considered SNR values so that the curve corresponding to the optimal route is a straight line over the SNR. It is seen that the optimal route requires much less energy than the longest path (almost one third in this case). Hence, we can improve the detection performance by choosing the path wisely, saving transmission energy significantly over the simple longest route approach which naively tries to maximize the expected innovation at each link.

5. CONCLUSIONS

We have considered a cross-layer approach to combine the network-layer routing with application performance directly for the detection of correlated random fields in multi-hop wireless sensor networks. We have proposed a link metric that captures the detection performance, and investigated its properties. Under the assumption of Gauss-Markov structure along a fusion route, we have shown that at high SNR the logarithm of innovation variance can be used as a link metric and the value of this metric is equivalent to the mutual information for Gaussian channel with signal power defined as the variance of signal innovation. We have also investigated the properties of the proposed metric. We have shown that for SNR > 1 the metric as a function of link length is strictly increasing, strictly concave, bounded from above and converging to $\frac{1}{2}\log(1+\text{SNR})$ as the link length increases unboundedly. We have also shown that the performance difference by the route shape is not significant when SNR is very low[2].

6. REFERENCES

[1] J. E. Wieselthier, G. D. Nguyen, and A. Ephremides, "On the construction of energy-efficient broadcast and multicast trees in wireless networks," in *INFOCOM 2000*, (Tel-Aviv, Israel), pp. 585 – 594, March 2000.

[2] S. Singh, M. Woo, and C. Raghavendra, "Power-aware routing in mobile ad hoc networks," in *Proc. 4th ACM/IEEE Conference on Mobile Computing and Networking (MobiCom)*, October 1998.

[3] H. Chang and L. Tassiulas, "Routing for maximum system lifetime in wireless ad-hoc networks," in *Proc. of the 37th Annual Allerton Conference on Communication, Control and Computing*, (Monticello, IL), Sep. 1999.

[4] S. Park and M. Srivastava, "Power aware routing in sensor networks using dynamic source routing," in *ACM MONET Special Issue on Energy Conserving Protocols in Wireless Networks*, 1999.

[5] J. Wiesselthier, G. Nguyen, and A. Ephremides, "Energy-aware wireless networking with directional antennas: The case of session-based broadcasting and multicasting," *IEEE Trans. Mob. Comput.*, vol. 1, no. 3, pp. 176 – 191, 2002.

[6] T. ElBatt and A. Ephremides, "Joint scheduling and power control for wireless ad-hoc networks," in *INFOCOM*, vol. 2, pp. 976 –984, 2002.

[7] T. Girici and A. Ephremides, "Joint routing and scheduling metrics for ad hoc wireless networks," in *Proc. of the 36th Asilomar Conference on Signals, Systems and Computers, 2002*, pp. 1155 – 1159, Nov. 2002.

[8] L. Yu and A. Ephremides, "Detection performance and energy-efficiency tradeoff in a sensor network ," in *Proc. of 2003 Allerton Conference*, (Allerton, IL), Oct. 2003.

[9] S. Pattem, B. Krishnamachari, and R. Govindan, "The impact of spatial correlation on routing with compression in wireless sensor networks," in *Proc. ACM/IEEE International Symposium on Information Processing in Sensor Networks (IPSN)*, (Berkeley, CA), April 2004.

[10] Y. Sung, L. Tong, and A. Ephremides, "Route selection for detection of correlated random fields in large sensor networks," in *2005 CISS*, (Baltimore, MD), March 2005.

[11] F. C. Schweppe, "Evaluation of likelihood functions for Gaussian signals," *IEEE Trans. on Information Theory*, vol. IT-1, pp. 61–70, 1965.

[12] H. V. Poor, *An Introduction to Signal Detection and Estimation*. New York: Springer-Verlag, 1994.

[13] H. Chernoff, "A measure of asymptotic efficiency for tests of a hypothesis based on the sum of observations," *Annals of Mathematical Statistics*, vol. 23, pp. 493–507, Dec. 1952.

[14] T. Kailath, A. H. Sayed, and B. Hassibi, *Linear Estimation*. Englewood Cliffs, NJ 07632: Prentice Hall, 2000.

[15] Y. Sung, *Detection of non-independent and identically distributed signals: Asymptotic analysis*. PhD thesis, Cornell University, Ithaca, NY, May 2005.

[2]The views and conclusions contained in this document are those of the authors and should not be interpreted as representing the official policies, either expressed or implied, of the Army Research Laboratory or the U.S. Government.